Linear and Nonlinear Unbalance Response of Cooper 8-Stage Compressor With A Squeeze Film Damper Support at the Non-Drive End

By
E. J. Gunter, Ph.D.
R. Armentrout, P.E.
P. Allaire, Ph.D.

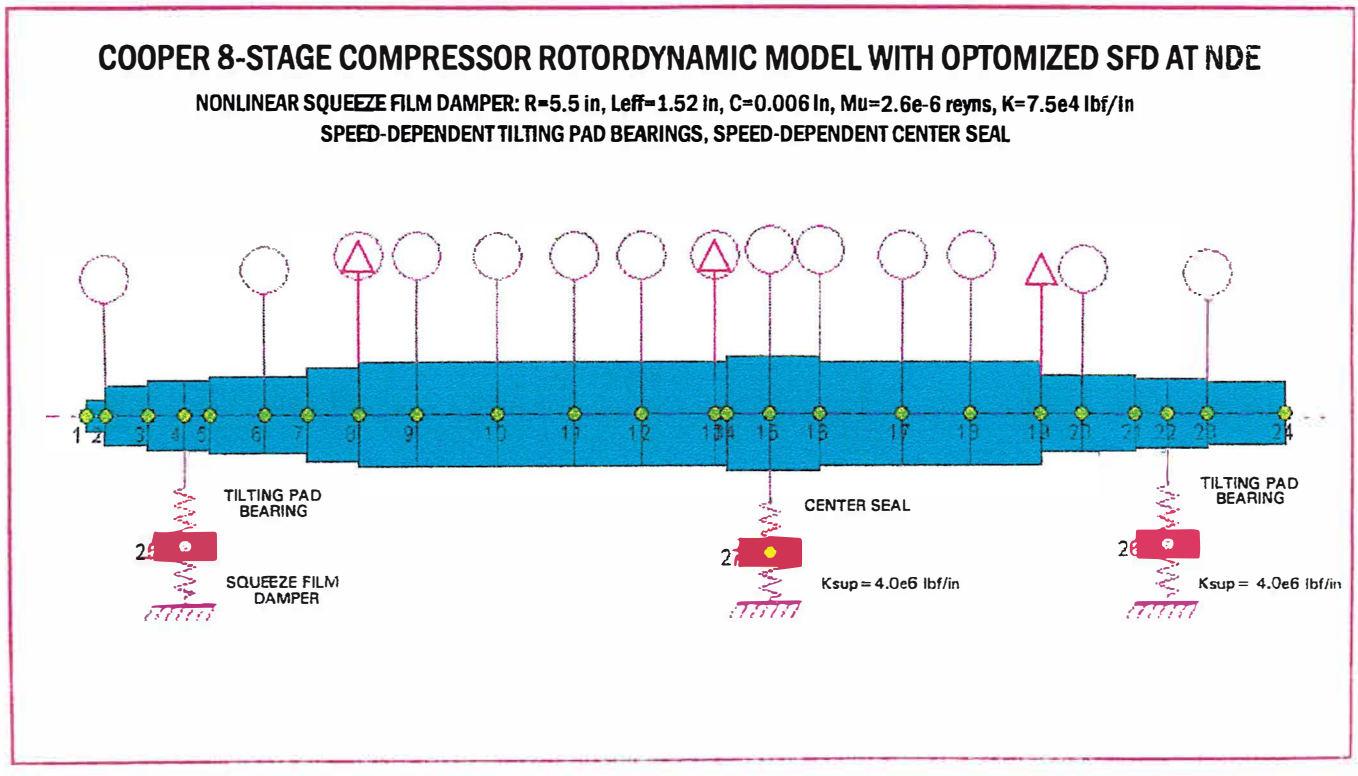

RODYN Vibration Analysis, Inc.
1932 Arlington Boulevard, Suite 223
Charlottesville, VA 22903-1560
(804) 296-3175

January, 1998

LIST OF FIGURES

1. BACKGROUND AND INTRODUCTION

The object of this report is to review the synchronous unbalance response of the eight-stage Cooper compressor with a squeeze film damper mounted at the non-drive end of the compressor. The principal objective of the squeeze film damper is to increase the log decrement of the compressor first mode to increase its stability characteristics. The squeeze film damper also has highly desirable effects on the unbalance response at running speed.

Figure 1.1, for example, represents the spectrum analysis of the Y motion at the free end of the eight-stage compressor during shutdown. This particular compressor exhibits an unusual self-excited instability phenomenon below the operating speed. As can been seen in the waterfall diagram, the self-excited instability appears to initiate at approximately 2,500 RPM and the subsynchronous whirl frequency tracks running speed. After passing through the rotor first critical speed around 4,000 RPM, the subsynchronous motion disappears.

This type of behavior in a centrifugal compressor in tilting pad bearings is highly unusual. Normally, self-excited whirl instability in a tilting pad rotor is initiated only when the rotor is operating well above its first critical speed. The whirl mechanism is usually caused by aerodynamic cross-coupling of the impellers and the balance piston. This does not appear to be the case. This type of whirl motion has been observed with floating bushing oil seals. It has also been observed that a supporting structure or foundation resonance can lead to a low frequency subsynchronous whirl motion. However, a pure structural mode does not normally track the rotor speed, as it appears to do in this case.

In addition to the observed self-excited whirl motion, it can be observed that the rotor amplitude at the Y probe is increasing with speeds above 5,000 RPM. This is caused by the rotor moving towards the second critical speed. Couple unbalance in the rotor will cause the ends to increase in amplitude above the first critical speed.

Figure 1.2 represents the synchronous response of the eight-stage compressor on start-up. The large jump at 3,900 RPM was due to a change in operating conditions. At speeds above 5,500 RPM, it is seen that the rotor synchronous amplitude increases. This is to be expected since the rotor is operating above the first critical speed and is approaching the rotor second critical speed. In the design of the combination of the tilting pad bearings and the squeeze film damper, both were optimized to provide the maximum rotor log decrement for the first forward

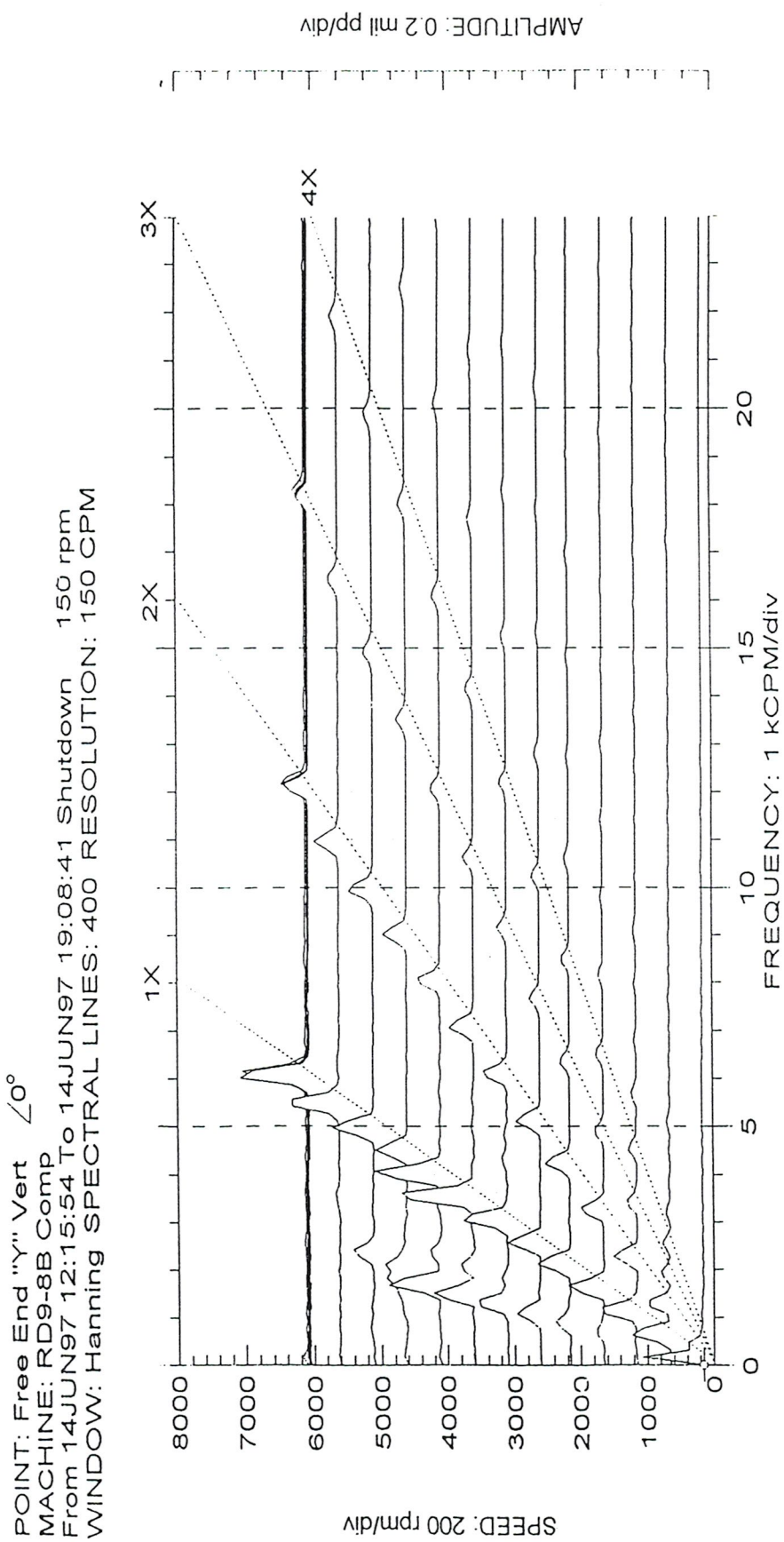

Figure 1.1 Spectrum Analysis of Y Motion at Free End of 8-Stage Compressor

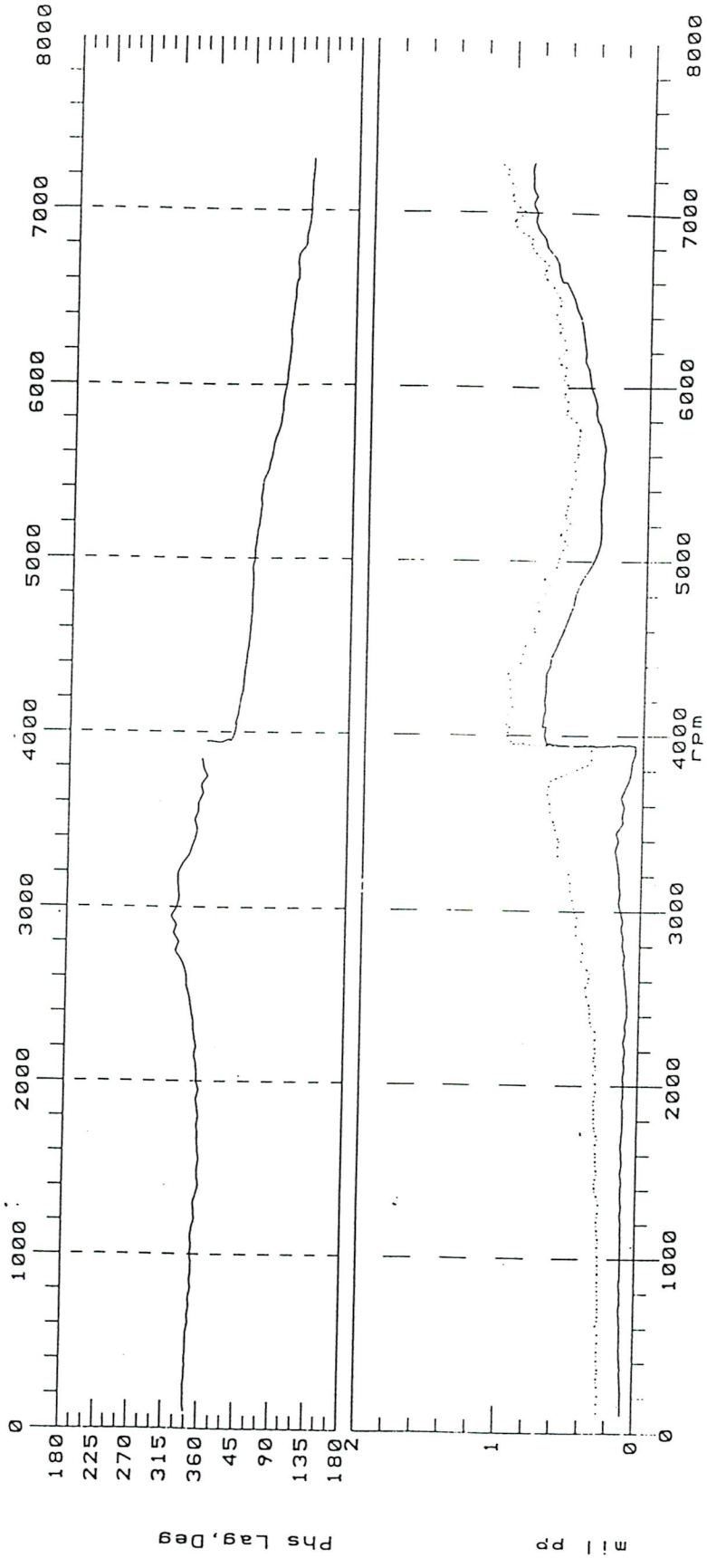

Figure 1.2 Synchronous Response of 8-Stage Compressor on Start-Up

critical speed. It was also observed that the introduction of the squeeze film damper increases the log decrement for the second critical speed, as well. The squeeze film damper improves the synchronous unbalance response characteristics of the rotor at running speed with static and couple unbalance distributions.

For example, the center labyrinth seal provides additional damping which is beneficial for the reduction of the amplitude at the first critical speed. However, since the center seal is near a node point for the second mode, it has only a negligible effect on the attenuation of the rotor second critical speed. However, the addition of a squeeze film damper at the non-drive end has a considerable influence on the attenuation of the rotor amplitude at the second critical speed. In general, it results in a reduction of the rotor response and also the bearing forces transmitted for a given unbalance distribution.

The unbalance response of the eight-stage compressor was analyzed assuming both linear and nonlinear squeeze film damper characteristics. For small displacements, the squeeze film damper may be evaluated as a linearized spring and damper system. The damping in a squeeze film damper remains relatively constant for eccentricities up to 40% of the damper clearance. The total stiffness of the SFD (squeeze film damper) is a combination of the mechanical spring rate of the O-ring plus the hydrodynamic stiffness generated by the damper. The hydrodynamic stiffness generated in a squeeze film damper varies from 0 at centered position and increases with the eccentricity of the orbit. However, for an orbital eccentricity of 40% or less of the bearing clearance, the main contribution of the stiffness for the SFD is provided by the supporting O-rings.

One of the areas of concern with the squeeze film damper is the response of the damper with large values of unbalance. With large values of unbalance, the rotor orbital motion about the origin can cause the squeeze film damper stiffness to become quite high. When the synchronous orbit in the damper exceeds 40% of the bearing clearance, the damper stiffness becomes highly nonlinear. Under these circumstances, a condition called damper lockup can occur in which the dynamic characteristics of the damper are no longer desirable under the large loading conditions.

In this report, both the linear and nonlinear responses of the rotor were analyzed with a wide range of unbalances, including both static and couple unbalance distributions. The ***DYROBES*** unbalance response program iterates on the nonlinear stiffness and damping generated in the squeeze film damper to determine the synchronous unbalance response. It was determined that the squeeze film damper behaves extremely well under a large range of unbalance.

Therefore, it is concluded that in addition to attenuating the first critical speed and increasing the log decrement for the first mode, the squeeze film damper also has highly desirable characteristics in attenuating the second critical speed and reducing the bearing forces transmitted at running speed for a generalized unbalance distribution containing both first and second mode unbalance distributions.

2. ROTOR UNBALANCE RESPONSE ON STIFF SUPPORTS

The rotor unbalance response for the eight-stage compressor was computed over a speed range from 1,000 to 8,000 RPM with three planes of unbalance. The unbalance distribution was chosen such that the first and third planes of unbalance represented a dynamic couple acting on the shaft. The second plane acting at the center was placed at 90° to the couple unbalance distribution. In this fashion, both first and second modal unbalance distributions are represented.

Figure 2.1 represents the 24-station finite element model of the eight-stage compressor. The circles on the figure represent major mass stations. The triangles drawn within the circle represent planes of unbalance. For example, the unbalance placed at stations 8 and 19 are 180° out of phase. The unbalance at station 13, which is near the rotor center, is 90° in phase from the unbalance at station 8. The rotor system is represented as a three-bearing system in order to include the effect of the center seal. The supporting structure under the tilting pad bearing and the center seal is assumed to be 4.0E6 lb/in stiffness.

Figure 2.2 represents the unbalance response of the eight-stage compressor at the bearings and mid-span without the squeeze film damper at the non-drive end. In this sample run, one oz-in unbalance was placed at each of the unbalance planes. The tilting pad bearing characteristics used are for the four-pad bearing and were assumed to be speed dependent, as shown in Table 2.1. In Figure 2.2, the amplitudes of motion are shown at stations 4, 14, and 22. These represent the first bearing, rotor center, and drive-end bearing, respectively. The largest amplitude of motion occurs at station 14 at 3,700 RPM. This represents the first resonant frequency. The amplitude at the rotor center is approximately two-and-a-half times larger than the amplitude at the bearing ends.

At a speed of approximately 6,000 RPM, the amplitude at the center span is of the same order of magnitude as the motion at the bearings. At speeds above 6,000 RPM, the center span amplitude is rapidly decreasing, while the motion at the bearing ends increases. The motion of the shaft near the center is similar to a single mass Jeffcott rotor passing through its critical speed. The amplitude at the bearing ends become out of phase as the rotor speed increases above the first critical speed. The motion at the bearing ends is relatively unaffected by the unbalance at station 13 near the rotor center. The amplitude of motion at the bearings above 6,000 RPM is controlled by the couple unbalance at stations 8 and 13.

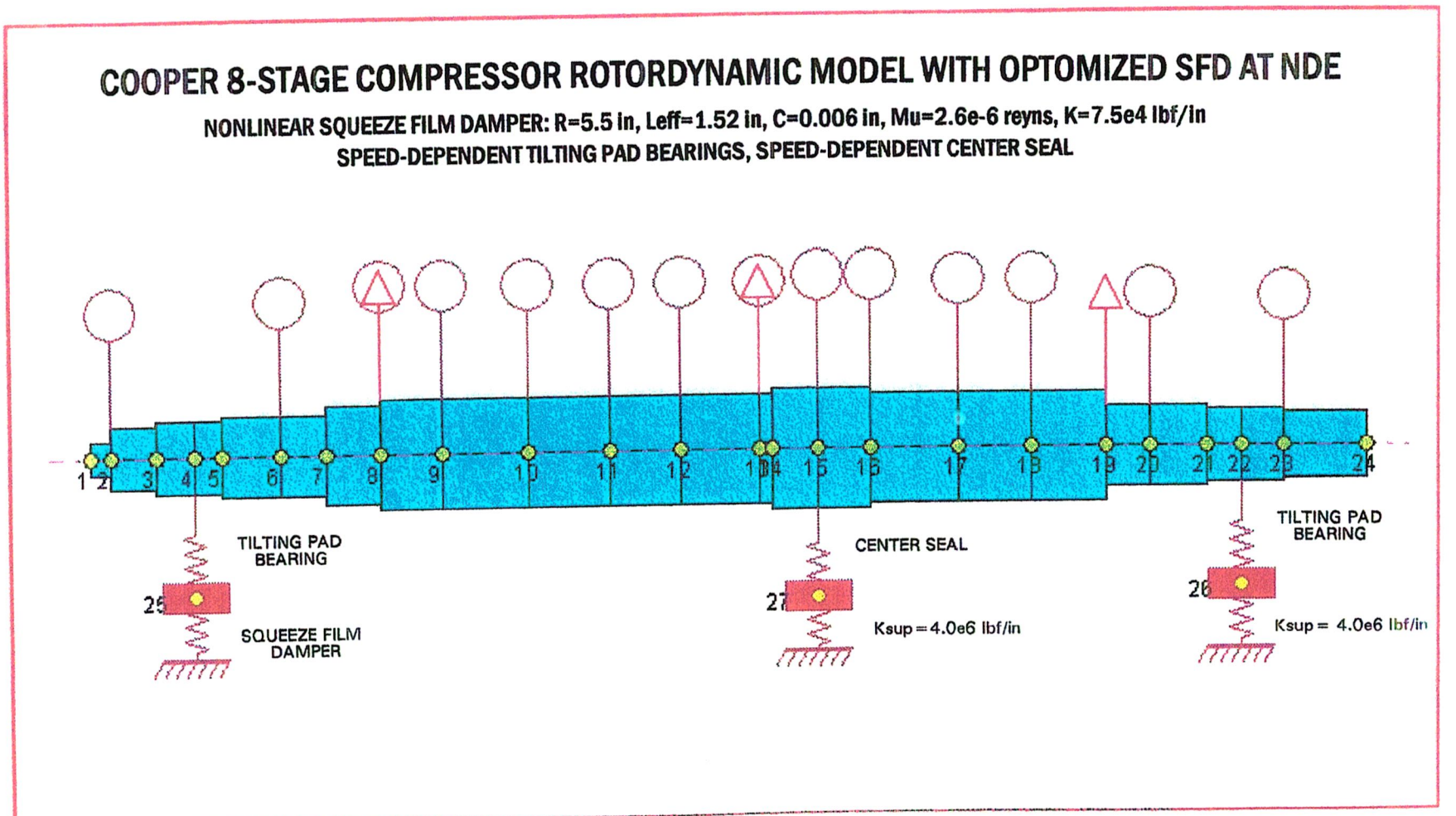

Figure 2.1 Finite Element Model of 8-Stage Compressor With Tilting Pad Bearings and a Squeeze Film Damper at the Non-Drive End

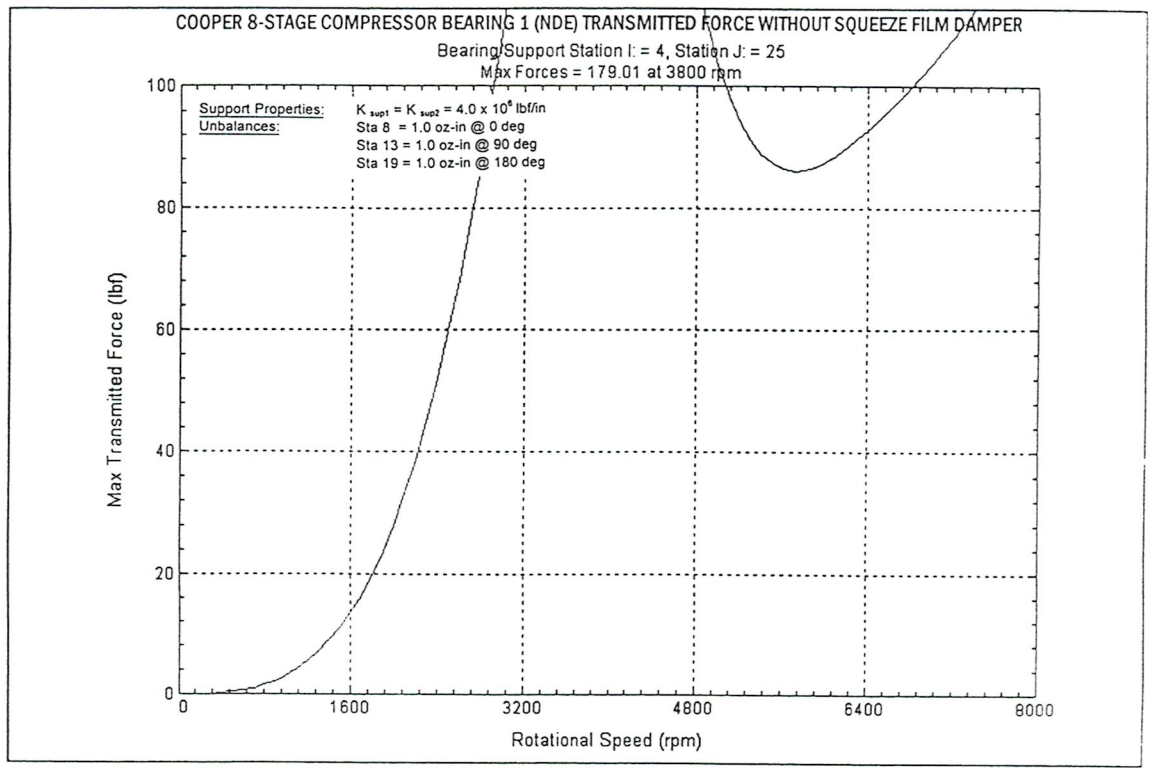

Figure 2.3 Transmitted Bearing Forces to the NDE Bearing With Tilting Pad Bearings on Stiff Support of $K_{support} = 4.0 \times 10^6$ lb/in

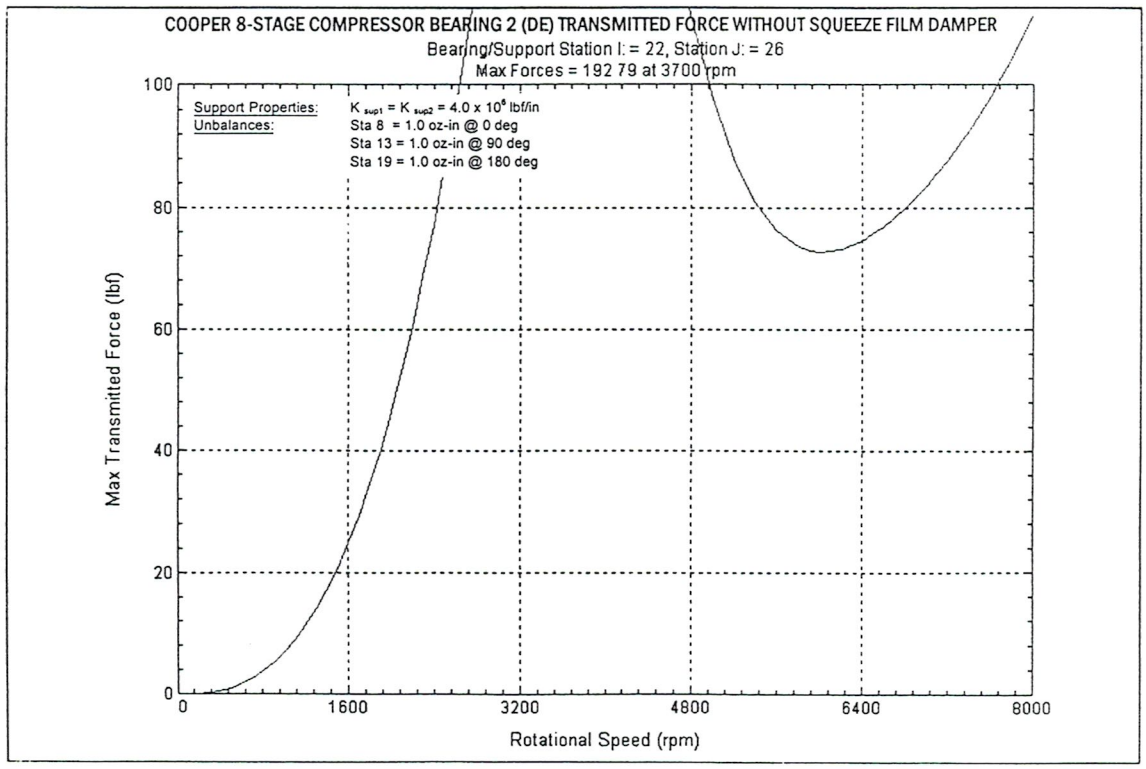

Figure 2.4 Transmitted Bearing Forces to the DE Bearing With Tilting Pad Bearings on Stiff Supports of $K_{support} = 4.0 \times 10^6$ lb/in

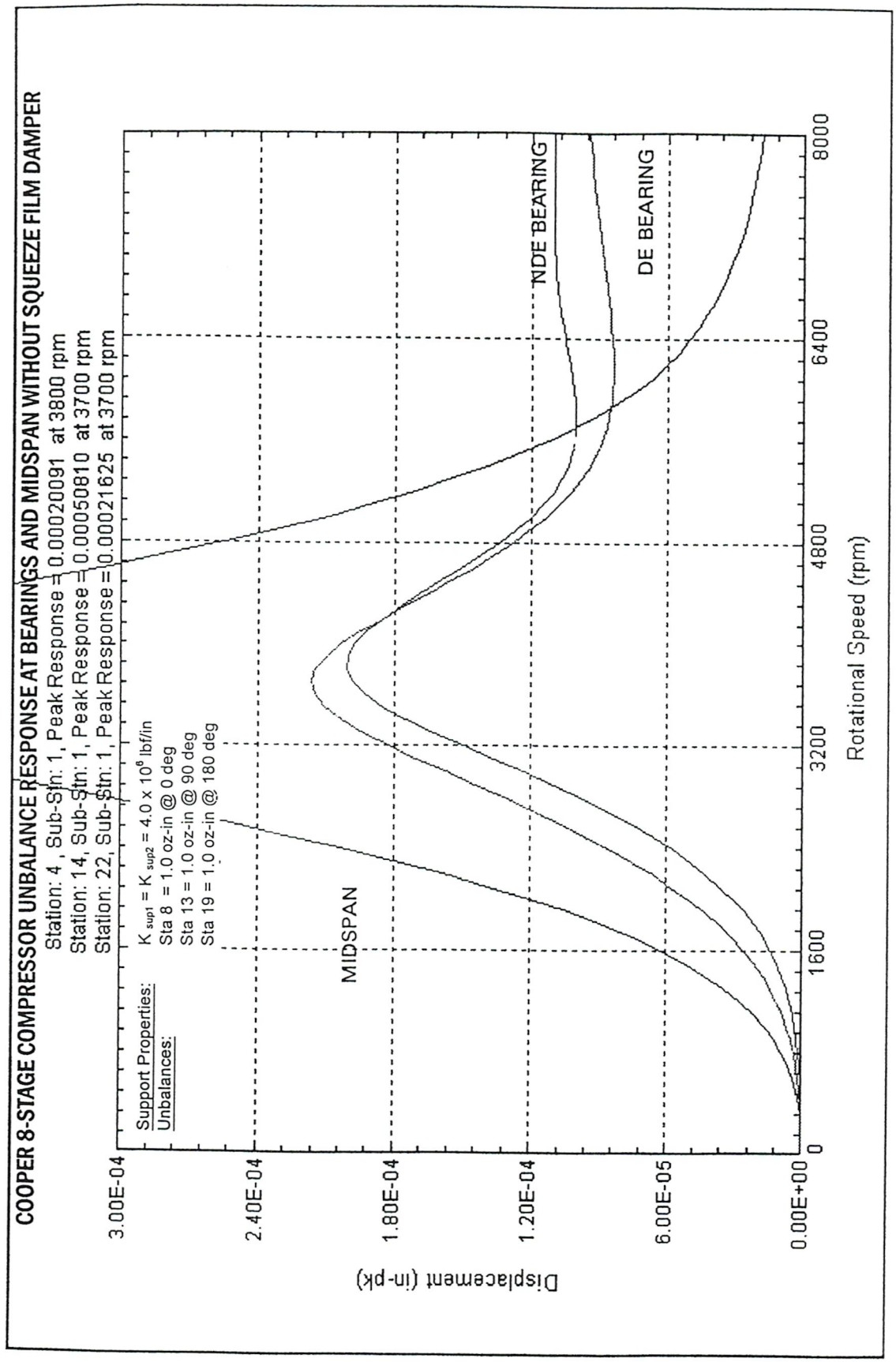

Figure 2.2 Response of 8-Stage Compressor at Bearings and Mid-Span Without Squeeze Film Damper at NDE With 3 Planes of Unbalance of 1.0 oz-in

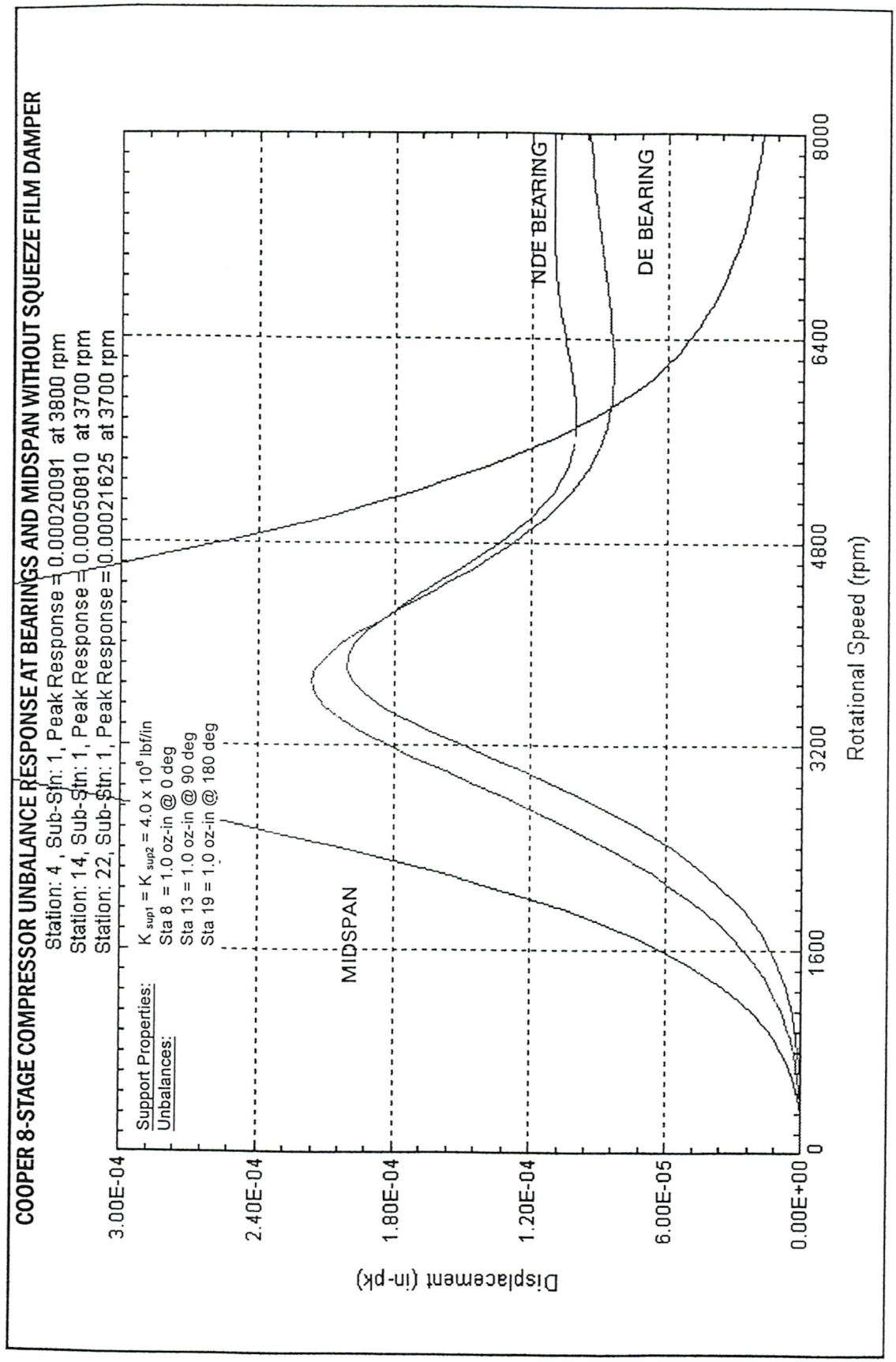

Figure 2.2 Response of 8-Stage Compressor at Bearings and Mid-Span Without Squeeze Film Damper at NDE With 3 Planes of Unbalance of 1.0 oz-in

Figures 2.3 and 2.4 represent the bearing forces transmitted at the non-drive end bearing (NDE) and also at the drive end bearing (DE), respectively. The maximum forces transmitted occur at 3,800 RPM and are 179 lb at the NDE bearing and 193 lb at the DE bearing. At 6,000 RPM, the bearing forces transmitted reduce to a minimum and then begin to increase. At 7,700 RPM, the bearing forces transmitted are approximately 100 lb per bearing. The rotating load generated by 1 oz-in at 7,700 RPM is 105.3 lb. Therefore, it is seen that the bearing forces transmitted above 6,000 RPM increase at a rate that is considerably greater than the rate of increase of the bearing amplitudes in this speed region.

Table 2.1 represents the ***DYROBES*** finite element model for the eight-stage compressor mounted in four-pad tilting bearings. The model consists of a shaft with 23 finite elements, four attached disks, and three bearing stations. At each bearing station is also considered a flexible support, as shown in Figure 2.1.

The bearing characteristics for the tilting pad bearing were computed by a separate program based on the nominal design bearing for the four-pad bearing for optimum damping. The bearing coefficients were computed for a speed range of 1,000 to 8,000 RPM. The computer program interpolates between speeds using a linear interpolation procedure. The tilting pad bearings for the non-drive and drive end were assumed to be identical, although they each carry a slightly different loading. The aerodynamic cross-coupling and seal damping were lumped at station 15. The seal damping and aerodynamic cross-coupling were also assumed to be speed dependent.

Table 2.1 shows the typical magnitude and location of the unbalance distribution for the rotor. Identical weights were placed at planes 8, 13, and 19. The center plane is rotated 90° from the first unbalance plane at station eight and the third unbalance plane is placed at 180° from station eight. This, in effect, produces a static and dynamic couple acting on the rotor. The dynamic component acts at a 90° vector to the static rotor unbalance forcing function. In this section for the simulation of the unbalance response on stiff supports, at identical foundation support stiffness values were used at all three bearing locations. These values were 4.0E6 lb/in for the bearing support stiffness values and an assumed damping of 0.1 lb-sec/in. It was found that the assumption of labyrinth seal stiffness and damping and also the assumed lumped aerodynamic cross-coupling acting at the center of the rotor had little effect on the rotor unbalance response when the rotor system was operating above the first critical speed.

Table 2.1 ***Dyrobes*** **Model of 8-Stage Compressor on Squeeze Film Bearings With Speed Dependent Bearing Coefficients**

```
FileName: C:\DyRoBeS\models\COOPRSD2.rot

************************************
**          Summary           **
**            of            **
**         input data         **
**            and            **
**       system parameters     **
************************************

      ***** Analysis Required *****

            Model Summary

**************************** System Parameters ****************************

           1  Shafts
          23  Elements
          23  SubElements
           4  Materials
          14  Rigid Disks
           3  Unbalances

           3  Linear Bearings
           1  NonLinear Bearings
           3  Flexible Supports

           0  Axial Loads
           0  Static Loads

           0  Natural Boundary Conditions
           6  Geometric Boundary Conditions
           6  Constraints

          27  Stations
         102  Degrees of Freedom

*****************************************************************************

**************************** Description Headers ****************************

8 STAGE COMPRESSOR - Qt=140,000
NOMINAL BEARINGS NDE & DE - Kxx=Kyy=5E5, Cxx=Cyy=1275
DE SUPPORT Kf=4E6, Cf=1E-1, Mf=2E-1
NDE SUPPORT Kf=4E6, Cf=0.1 base design case
CENTER SEAL DAMPING

*****************************************************************************
```

Table 2.1 (Continued)

********** Material Properties **********

Property no	Mass Density	Elastic Modulus	Shear Modulus
1	.73550E-03	.29000E+08	.11500E+08
2	.41700E-03	.15500E+08	.65000E+07
3	.25900E-03	.10000E+08	.38000E+07
4	.67300E-03	.14500E+08	.60000E+07

****

********** Shaft Elements **********

Ele no	Sub Ele no	Left End Loc	Length	Mass Inner Diameter	Mass Outer Diameter	Stiffness Inner Diameter	Stiffness Outer Diameter	Material no
1	1	.000	1.7500	.0000	2.9600	.0000	2.9600	1
2	1	1.750	3.9500	.0000	5.4000	.0000	5.4000	1
3	1	5.700	3.2900	.0000	6.4800	.0000	6.4800	1
4	1	8.990	2.4000	.0000	6.4800	.0000	6.4800	1
5	1	11.390	4.9500	.0000	7.0000	.0000	7.0000	1
6	1	16.340	3.8100	.0000	7.0000	.0000	7.0000	1
7	1	20.150	4.8100	.0000	8.7200	.0000	8.7200	1
8	1	24.960	5.2200	.0000	9.4600	.0000	9.4600	1
9	1	30.180	7.3700	.0000	9.4600	.0000	9.4600	1
10	1	37.550	7.0000	.0000	9.4600	.0000	9.4600	1
11	1	44.550	6.0700	.0000	9.4600	.0000	9.4600	1
12	1	50.620	6.6900	.0000	9.4600	.0000	9.4600	1
13	1	57.310	1.0900	.0000	9.4600	.0000	9.4600	1
14	1	58.400	4.0200	.0000	10.4200	.0000	10.4200	1
15	1	62.420	4.4500	.0000	10.4200	.0000	10.4200	1
16	1	66.870	7.4900	.0000	9.4600	.0000	9.4600	1
17	1	74.360	6.2500	.0000	9.4600	.0000	9.4600	1
18	1	80.610	6.3600	.0000	9.4600	.0000	9.4600	1

Table 2.1 (Continued)

```
19
  1  86.970  3.8000   .0000  7.0000   .0000  7.0000   1
20
  1  90.770  4.7900   .0000  7.0000   .0000  7.0000   1
21
  1  95.560  2.9800   .0000  6.4800   .0000  6.4800   1
22
  1  98.540  3.6400   .0000  6.4800   .0000  6.4800   1
23
  1 102.180  7.0000   .0000  5.8600   .0000  5.8600   1
```

********** Rigid Disks **********

Stn no	Mass	Diametral Inertia	Polar Inertia
2	.71760E-01	.59720	1.1943
6	.11530	1.0050	2.0100
8	.10750E-01	.13150	.26300
9	.43240	16.387	32.773
10	.43190	15.076	30.152
11	.37820	13.946	27.892
12	.37600	13.637	27.273
13	.34610	12.688	25.377
15	.50520E-01	.73700	1.4740
16	.23380	5.8569	11.714
17	.24720	6.4644	12.929
18	.27110	7.5104	15.021
20	.11530	1.0052	2.0100
23	.25910	2.2111	4.4220

********** Rotor Equivalent Rigid Body Properties **********

Rotor no	Left End Location	Length	C.M. Location	Diametral Mass	Polar Inertia	Speed Inertia	Ratio
1	.000	109.180	54.921	7.8537	5113.7	240.1	1.0000

********** Bearing Coefficients **********

Stnl, J	Angle	rpm	Coefficients			
4 25	.00		(Speed Dependent Coefficients)			
		1000.00				
Kxx Kxy Kyx Kyy			.106000E+07	.000000	.000000	.106000E+07
Cxx Cxy Cyx Cyy			7551.00	.000000	.000000	7551.00
Krr Krs Ksr Krr			.000000	.000000	.000000	.000000
Crr Crs Csr Crr			.000000	.000000	.000000	.000000
		2000.00				
Kxx Kxy Kyx Kyy			797000.	.000000	.000000	797000.
Cxx Cxy Cyx Cyy			3819.00	.000000	.000000	3819.00
Krr Krs Ksr Krr			.000000	.000000	.000000	.000000

Table 2.1 (Continued)

```
Crr Crs Csr Crr     .000000     .000000     .000000     .000000
          3000.00
Kxx Kxy Kyx Kyy     675000.     .000000     .000000     675000.
Cxx Cxy Cyx Cyy     2616.00     .000000     .000000     2616.00
Krr Krs Ksr Krr     .000000     .000000     .000000     .000000
Crr Crs Csr Crr     .000000     .000000     .000000     .000000
          4000.00
Kxx Kxy Kyx Kyy     599000.     .000000     .000000     599000.
Cxx Cxy Cyx Cyy     2022.00     .000000     .000000     2022.00
Krr Krs Ksr Krr     .000000     .000000     .000000     .000000
Crr Crs Csr Crr     .000000     .000000     .000000     .000000
          7000.00
Kxx Kxy Kyx Kyy     481000.     .000000     .000000     481000.
Cxx Cxy Cyx Cyy     1323.00     .000000     .000000     1323.00
Krr Krs Ksr Krr     .000000     .000000     .000000     .000000
Crr Crs Csr Crr     .000000     .000000     .000000     .000000
          8000.00
Kxx Kxy Kyx Kyy     506000.     .000000     .000000     506000.
Cxx Cxy Cyx Cyy     1534.00     .000000     .000000     1534.00
Krr Krs Ksr Krr     .000000     .000000     .000000     .000000
Crr Crs Csr Crr     .000000     .000000     .000000     .000000

 25   0    .00          (Squeeze Film Damper)

C                                 R           L           Cr              mu- REYNS
 SFR SFL SFC SFV    5.00000     1.30000     .350000E-02 .100000E-05
C                                Ksup        Csup
 SFC K SFCC         200000.     .100000E-01 .000000     .000000

 22  26    .00          (Speed Dependent Coefficients)

          1000.00
Kxx Kxy Kyx Kyy     .106000E+07 .000000     .000000     .106000E+07
Cxx Cxy Cyx Cyy     7551.00     .000000     .000000     7551.00
Krr Krs Ksr Krr     .000000     .000000     .000000     .000000
Crr Crs Csr Crr     .000000     .000000     .000000     .000000
          2000.00
Kxx Kxy Kyx Kyy     797000.     .000000     .000000     797000.
Cxx Cxy Cyx Cyy     3819.00     .000000     .000000     3819.00
Krr Krs Ksr Krr     .000000     .000000     .000000     .000000
Crr Crs Csr Crr     .000000     .000000     .000000     .000000
          3000.00
Kxx Kxy Kyx Kyy     675000.     .000000     .000000     675000.
Cxx Cxy Cyx Cyy     2616.00     .000000     .000000     2616.00
Krr Krs Ksr Krr     .000000     .000000     .000000     .000000
Crr Crs Csr Crr     .000000     .000000     .000000     .000000
          4000.00
Kxx Kxy Kyx Kyy     599000.     .000000     .000000     599000.
Cxx Cxy Cyx Cyy     2022.00     .000000     .000000     2022.00
Krr Krs Ksr Krr     .000000     .000000     .000000     .000000
Crr Crs Csr Crr     .000000     .000000     .000000     .000000
          7000.00
Kxx Kxy Kyx Kyy     481000.     .000000     .000000     481000.
```

Table 2.1 (Continued)

```
Cxx Cxy Cyx Cyy      1323.00    .000000    .000000    1323.00
Krr Krs Ksr Krr       .000000    .000000    .000000    .000000
Crr Crs Csr Crr       .000000    .000000    .000000    .000000
        8000.00
Kxx Kxy Kyx Kyy      506000.    .000000    .000000    506000.
Cxx Cxy Cyx Cyy      1534.00    .000000    .000000    1534.00
Krr Krs Ksr Krr       .000000    .000000    .000000    .000000
Crr Crs Csr Crr       .000000    .000000    .000000    .000000

 15  27    .00          (Speed Dependent Coefficients)

        4000.00 ( ASSUMED AERODYNAMIC CROSS COUPLING)
Kxx Kxy Kyx Kyy       .000000   .700000E+07 -70000.0    .000000
                  (ASSUMED SEAL DAMPING )
Cxx Cxy Cyx Cyy      200.000    .000000    .000000    200.000
Krr Krs Ksr Krr       .000000    .000000    .000000    .000000
Crr Crs Csr Crr       .000000    .000000    .000000    .000000
        8000.00
                  ( AERODYNAMIC CROSS COUPLING )
Kxx Kxy Kyx Kyy       .000000   140000.   -140000.    .000000
                  ( SEAL DAMPING )
Cxx Cxy Cyx Cyy      400.000    .000000    .000000    400.000
Krr Krs Ksr Krr       .000000    .000000    .000000    .000000
Crr Crs Csr Crr       .000000    .000000    .000000    .000000

*******************************************************************************

*************************** Unbalance (M x Ecc) ****************************
  Ele  SubEle    ----- Left End -----       ----- Right End ----
   no    no      Magnitude    Angle       Magnitude    Angle
                (24 OZ-IN UNBALANCE IN 3 PLANES EACH)
    8     1     .38800E-02     .00          .00000       .00
   13     1     .38800E-02   90.00          .00000       .00
   19     1     .38800E-02  180.00          .00000       .00

*******************************************************************************

*************************** Flexible Supports ****************************
 Stnl          ---------- Coefficients ----------
  25
Mxx Mxy Myx Myy   .100000E-01  .000000    .000000    .100000E-01
Cxx Cxy Cyx Cyy     1.00000    .000000    .000000    1.00000
Kxx Kxy Kyx Kyy     1.00000    .000000    .000000    1.00000
  26
Mxx Mxy Myx Myy   .200000    .000000    .000000    .200000
Cxx Cxy Cyx Cyy   .100000    .000000    .000000    .100000
Kxx Kxy Kyx Kyy   .400000E+07  .000000    .000000    .400000E+07
  27
Mxx Mxy Myx Myy   .100000    .000000    .000000    .100000
Cxx Cxy Cyx Cyy   .100000    .000000    .000000    .000000
Kxx Kxy Kyx Kyy   .400000E+07  .000000    .000000    .400000E+07

*******************************************************************************
```

3. ROTOR UNBALANCE RESPONSE IN NONLINEAR SQUEEZE FILM DAMPER AT NON-DRIVE END BEARING

The unbalance response of the eight-stage compressor was analyzed with a nonlinear squeeze film damper placed at the non-drive end bearing. The design of the squeeze film damper used in the calculations has a radial clearance of C_r=6 mils, an effective damper length of L=1.52 inches, and damper radius of R=5.5 inches. The oil viscosity used was assumed to be μ=2.6E-6 reyns. The spring rate supporting the squeeze film damper generated by the O-rings was assumed to be K_d=75,000 lb/in. The support assumed acting at the center seal and the drive end bearing was assumed to be K_s=4.0E6 lb/in.

For small values of damper displacement or eccentricity, the damping characteristics may be considered constant. The squeeze film damping does not begin to increase until eccentricities exceeding .4 are achieved. The squeeze film damper for small displacements produces four damping coefficients. For the assumption of circular synchronous orbiting about the origin, the cross-coupled damping coefficients act as radial stiffness terms. These coefficients vary nonlinearly as a function of eccentricity. Above values of ϵ=.4, the effective stiffness of the damper begins to increase dramatically. The characteristics of the squeeze film damper are given in Appendix A.

In the normal unbalance response analysis, the supporting structure is assumed to be linear. That is, if one should double the rotating unbalance acting on the shaft, then the unbalance response would be proportional. With a squeeze film damper, this is not the case, since the damper characteristics are nonlinear. The orbital motion of the damper must remain within the damper clearance. At very high levels of unbalance, a situation referred to as "damper lockup" may occur. Under these circumstances, the damper is orbiting at 80–90% of the damper clearance and the system acts as a very stiff spring. Under these circumstances, the dynamic characteristics of the damper system may be highly undesirable.

In this phase of the analysis, the shaft unbalance response was analyzed for three levels of rotating unbalance. The first level was an unbalance distribution of 1 oz-in unbalance placed at the three planes along the rotor. In the calculation of the nonlinear response of the shaft, it is assumed that the damper motion is in a synchronous circular orbit about the bearing origin. This is a reasonable assumption for most situations. To compute a solution, the program must iterate on the nonlinear stiffness and damping forces to determine an equilibrium solution for

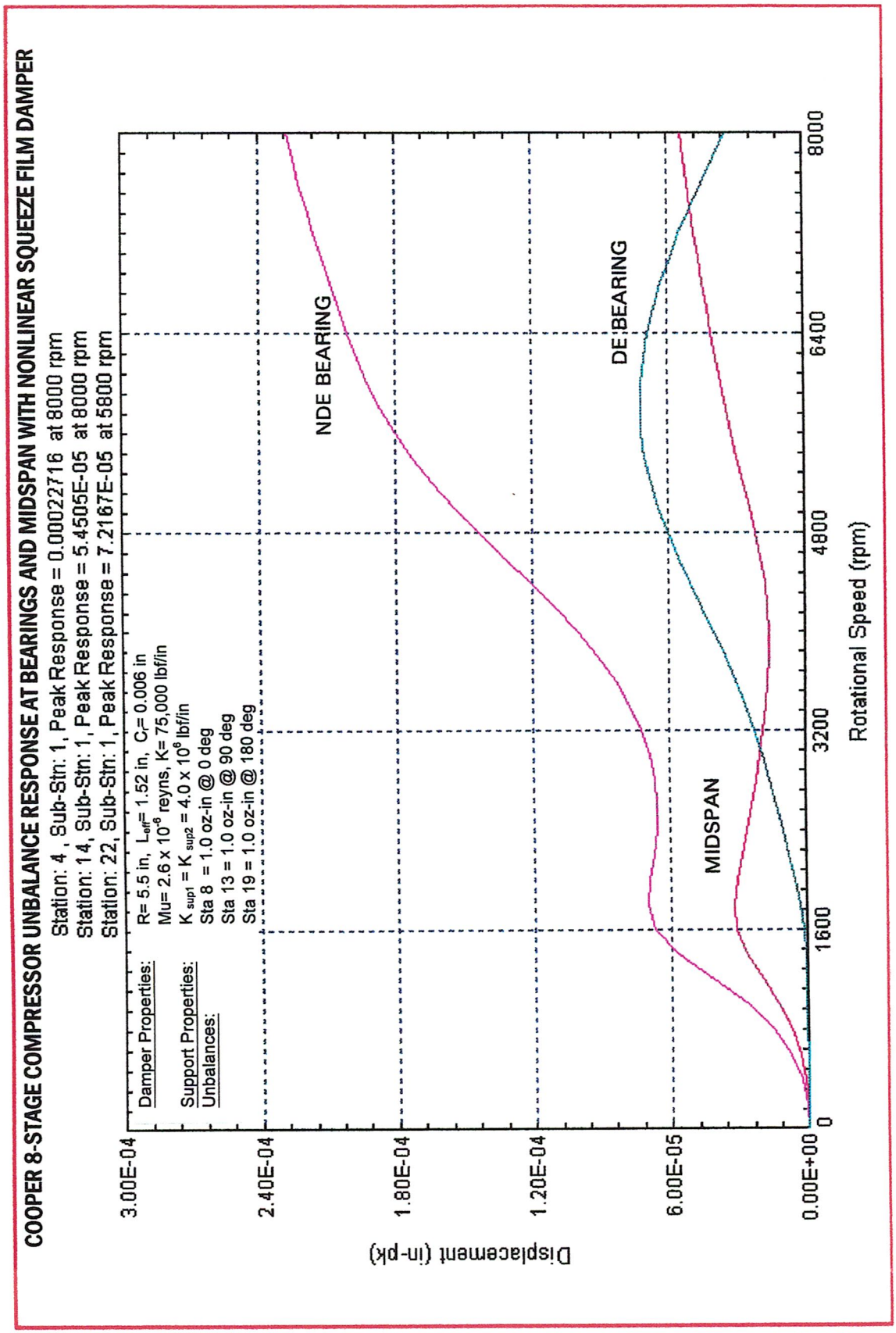

Figure 3.1 Unbalance Response of 8-Stage Compressor in Nonlinear Squeeze Film Damper at NDE With 3 Planes of Unbalance of 1.0 oz-in

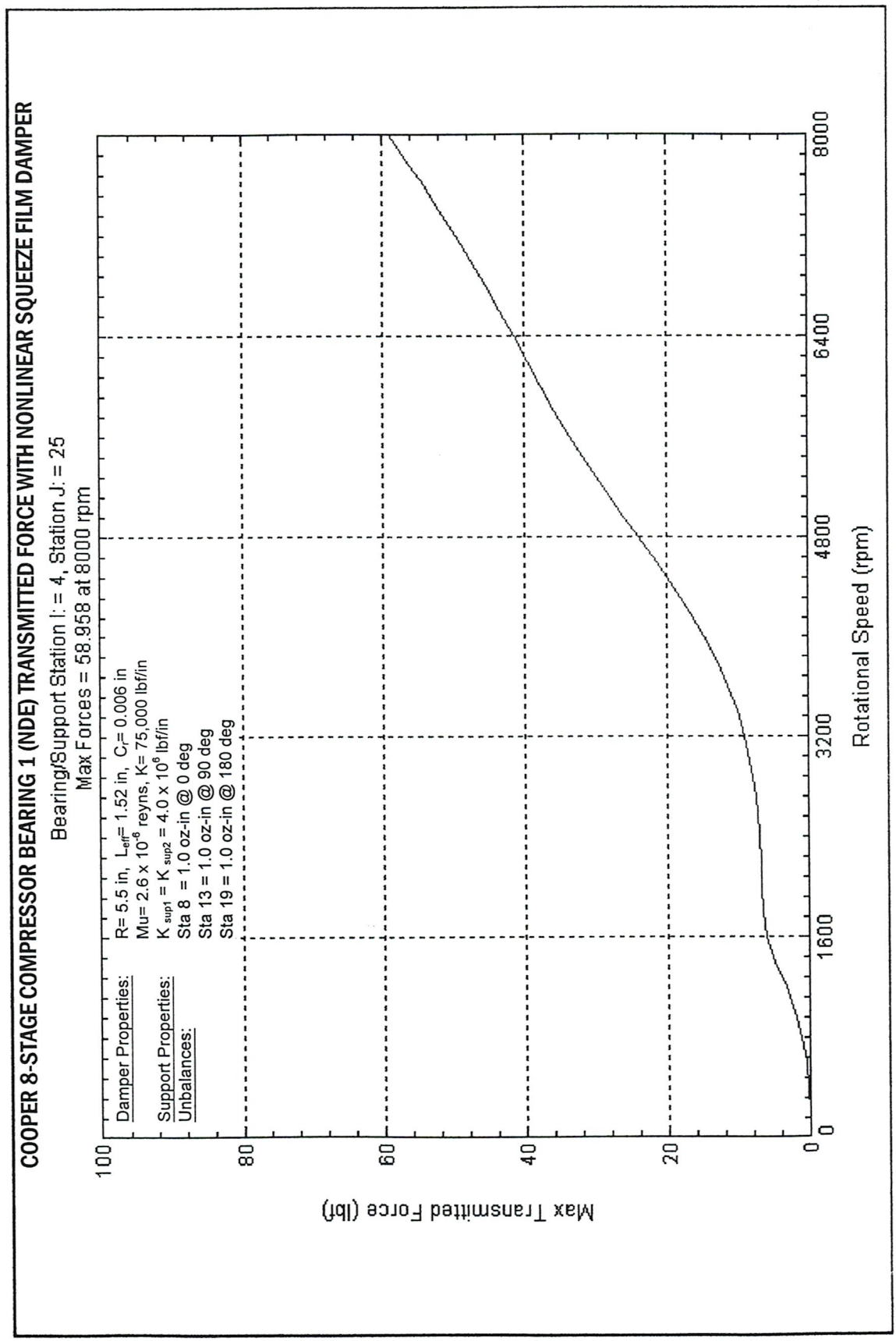

Figure 3.2 Transmitted Bearing Forces to NDE Bearing With Nonlinear Squeeze Film Damper and 3 Planes of Unbalance of 1.0 oz-in

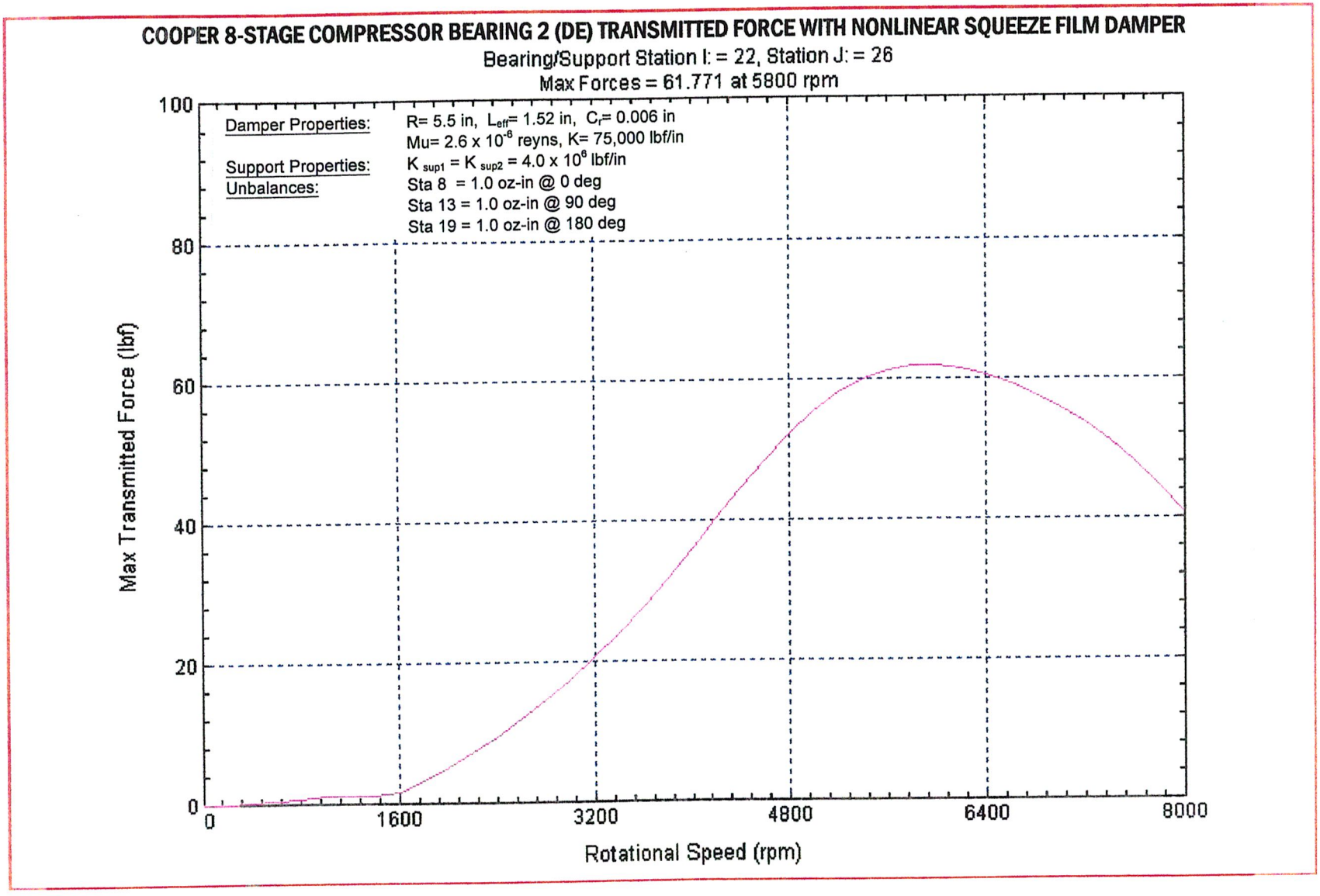

Figure 3.3 Transmitted Bearing Forces to DE Bearing With Nonlinear Squeeze Film Damper at NDE and 3 Planes of Unbalance of 1.0 oz-in

a particular speed. Therefore, the nonlinear lateral response calculations are considerably more time consuming. Figure 3.1 represents the unbalance response of the eight-stage compressor with three planes of unbalance of 1.0 oz-in. The motion is shown for the mid-span, the NDE bearing, and the drive end (DE) bearing. Note that the squeeze film damper has caused a dramatic reduction of the center span amplitude, as compared to Figure 2.2. In Figure 2.2, the amplitude at 3,700 RPM is 5E-4 in. The maximum amplitude occurs now at 8,000 RPM and is 5.4E-5 in.

The squeeze film damper has reduced the first critical to approximately 1,800 RPM. The amplitude along the rotor at the first critical is now higher at the NDE bearing, 7E-5 in, as compared to 3.0E-5 at the shaft center. The mode shape for the rotor at 2,400 RPM is shown in Figure 3.5A. The drive-end bearing motion is very small, with a conical motion about the non-drive end bearing. Thus, the single squeeze film damper at the non-drive end is extremely effective in attenuating the unbalance response at the critical speed.

As the speed increases, the amplitude at the non-drive end bearing continues to increase and reaches a maximum at 8,000 RPM. Figure 3.1 shows that the maximum motion at the NDE bearing at 8,000 RPM is higher than what would be encountered with the bearing on the stiff supports. However, the bearing forces transmitted have been reduced.

Figure 3.2 represents the transmitted bearing forces to the NDE bearing with the nonlinear squeeze film damper and three planes of unbalance of 1.0 oz-in. The maximum force transmitted at 8,000 RPM is 59 lb, as compared to the over 120 lb transmitted as shown in Figure 2.3. Thus, the NDE squeeze film damper has reduced the bearing forces transmitted by over one-half. Even though the rotor motion may be larger with the squeeze film damper at the NDE bearing, the actual bearing forces transmitted will be half of the original values because of the reduced support stiffness and increased damping.

Figure 3.3 represents the transmitted bearing forces to the drive end bearing with the nonlinear squeeze film damper at NDE and three planes of unbalance of 1.0 oz-in. Figure 3.3 shows that the maximum force has a peak value of 62 lb at 5,800 RPM. This also corresponds with the peak amplitude as observed in Figure 3.1. It is of interest to note that the drive end bearing forces reduce above 5,800 RPM, whereas the non-drive end forces continue to increase.

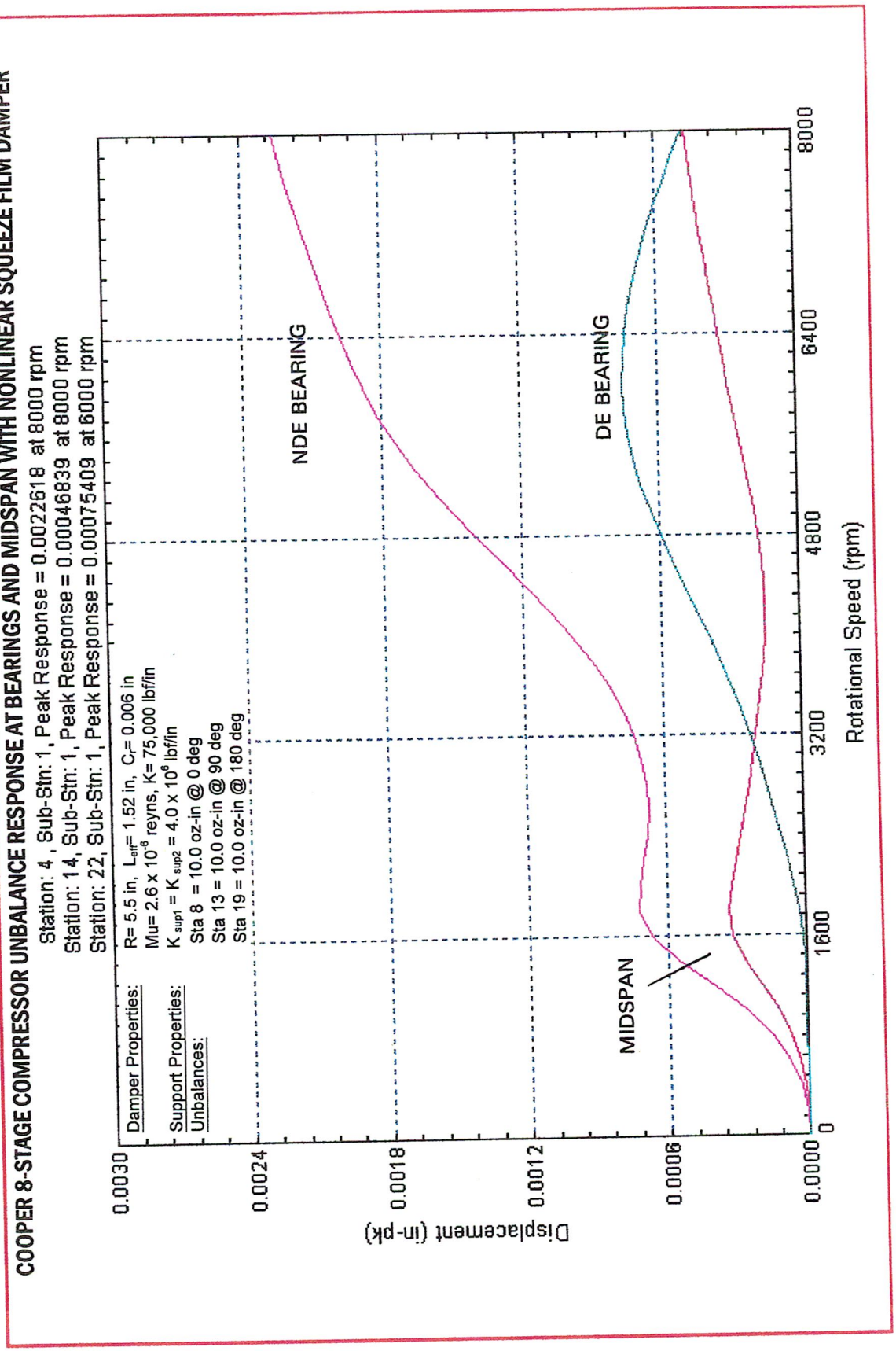

Figure 3.4 Unbalance Response of 8-Stage Compressor in Nonlinear Squeeze Film Damper at NDE With 3 Planes of Unbalance of 10.0 oz-in

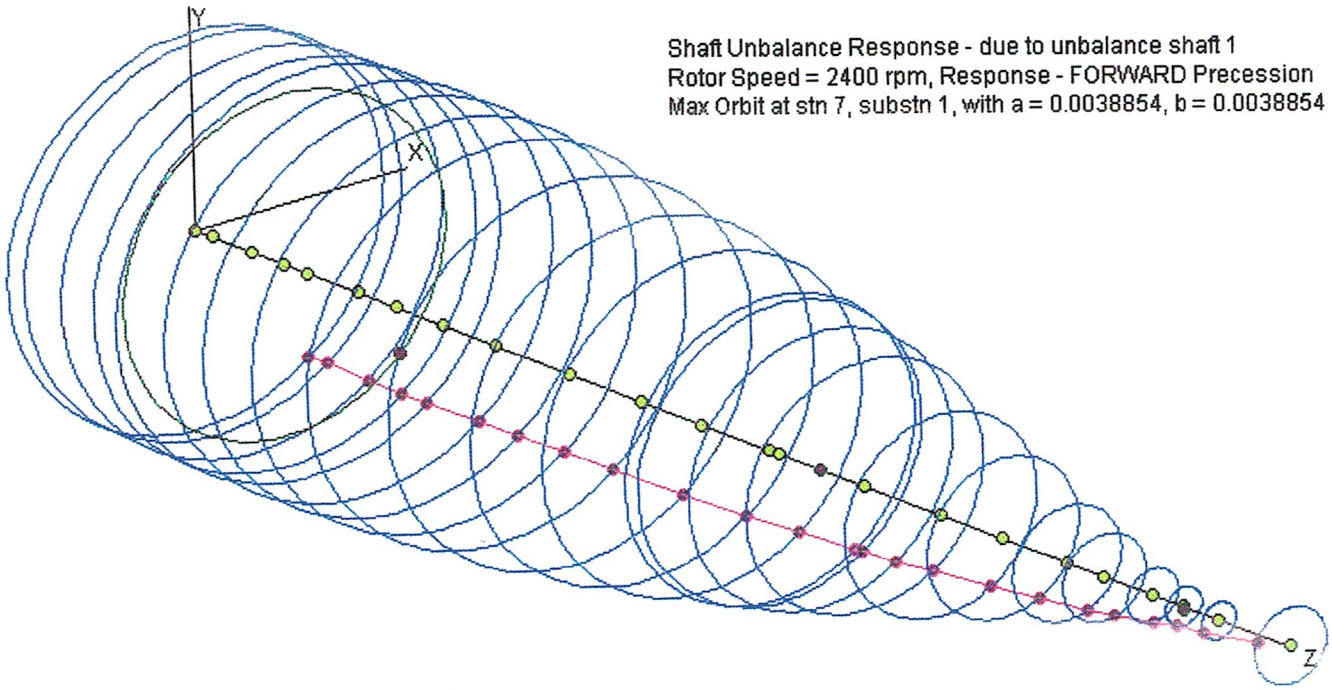

Figure 3.5A Rotor Unbalance Response Mode Shape at 2,400 RPM- 1st Mode

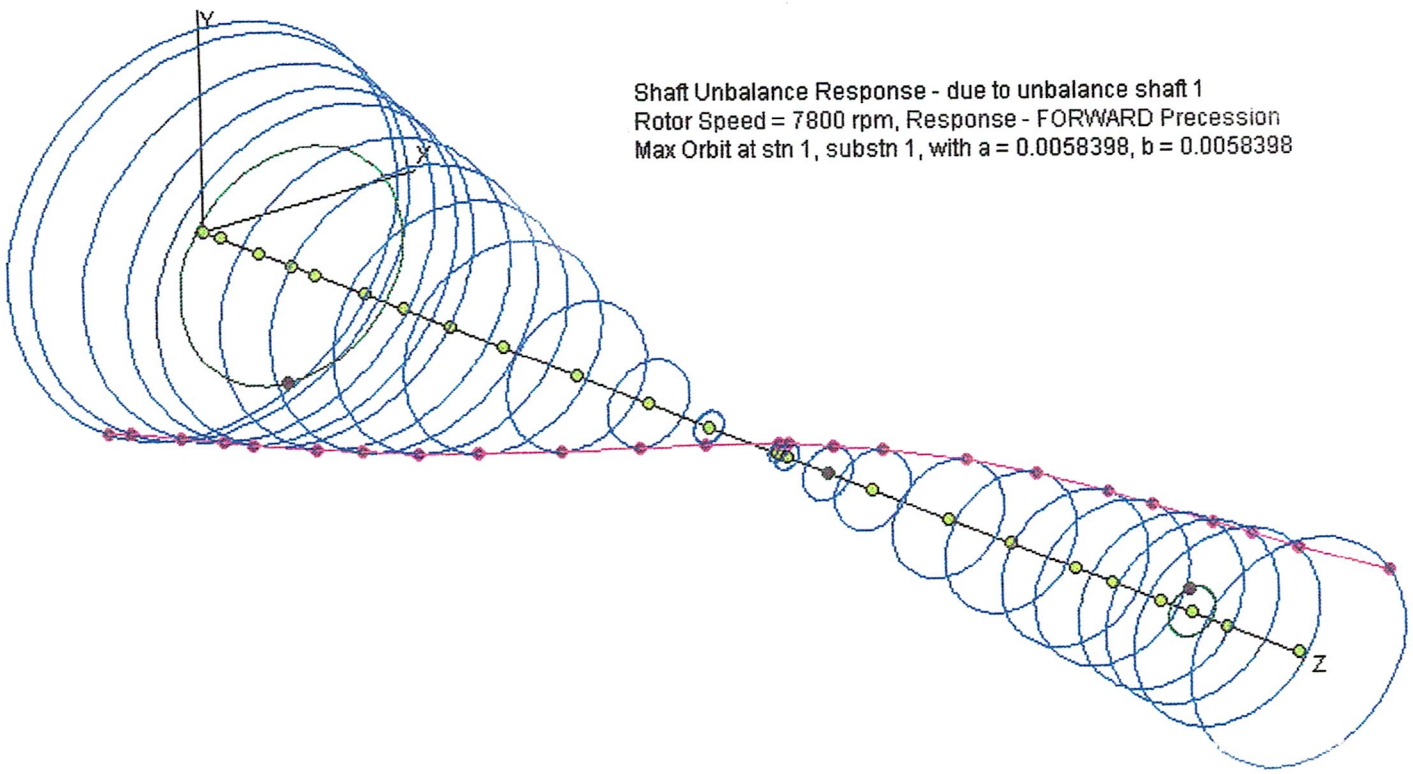

Figure 3.5B Rotor Unbalance Response Mode Shape at 7,800 RPM

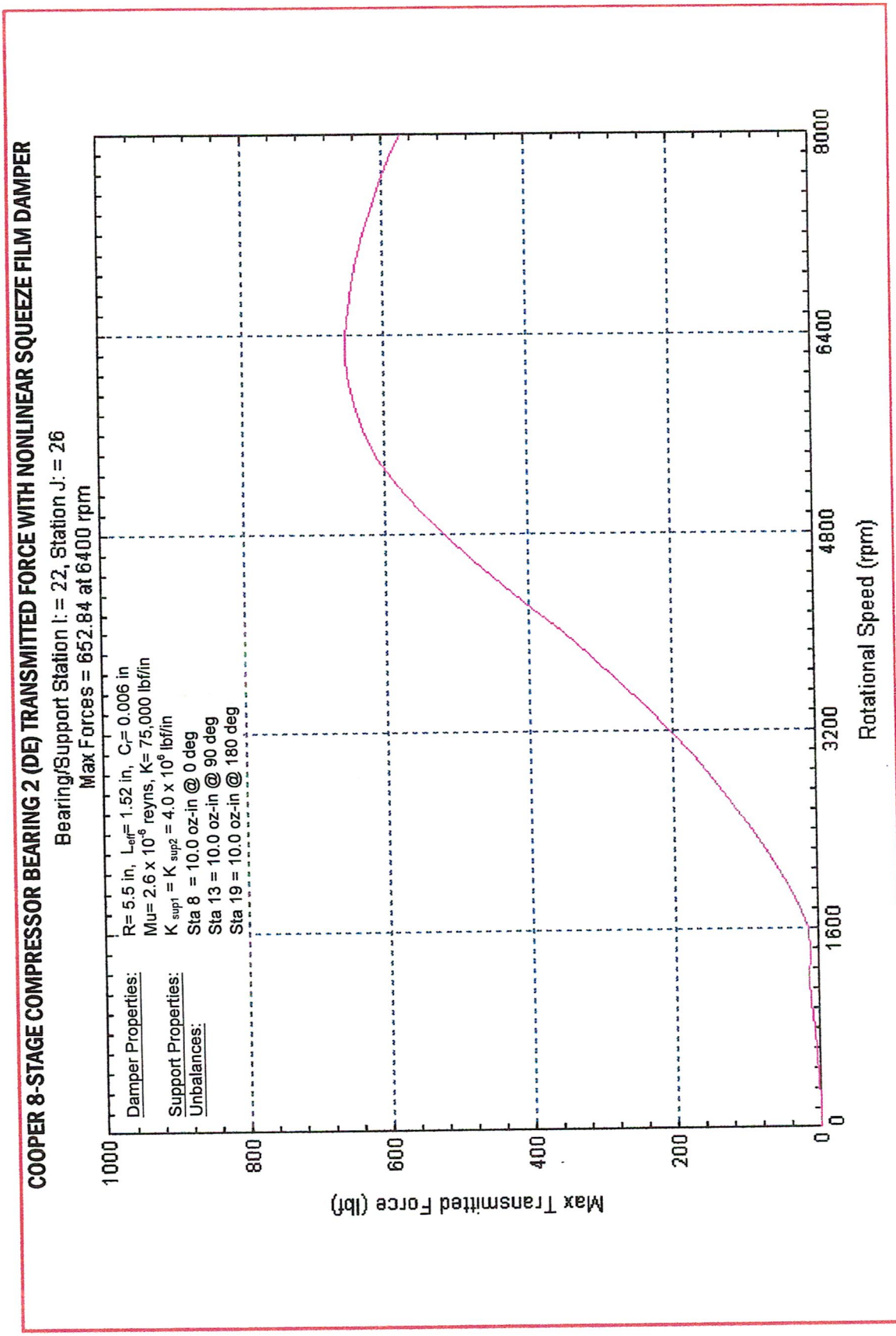

Figure 3.6 Drive End Transmitted Bearing Forces With 3 Planes of Unbalance of 10.0 oz-in

Figure 3.4 represents the unbalance response at the mid-span and bearings with the unbalance increased by a factor of 10, to 10.0 oz-in at each of the three unbalance planes. The response due to the ten-fold increase is fairly linear, as can be observed by the comparison of Figure 3.5 with Figure 3.1 on the response with 1 oz-in unbalance. The rotor is well behaved with the unbalance distribution of 10 oz-in and does not exhibit any indication of damper lockup.

Figure 3.5A and Figure 3.5B represent the rotor unbalance response mode shapes at 2,400 RPM and 7,800 RPM, respectively. The form of the mode shapes remains similar for the three ranges of unbalances computed. Figure 3.5 shows that at 2,400 RPM the response at all stations is essentially in phase. The largest orbit occurs at station 7 near the non-drive end bearing. The coupling motion at station 24 is approximately a node point with little motion. At the running speed of 7,800 RPM, the mode shape has changed dramatically, with the bearings out of phase. The motion is essentially a conical motion, with the largest orbit at station 1. There is an inside orbit drawn at the fourth station which represents the motion of the squeeze film damper. Station 13 has zero motion and is a nodal point. The center seal is acting at approximately station 15. Hence, the damping provided by the center seal will have little effect on the attenuation of the rotor at running speed.

Figure 3.6 represents the forces transmitted to the drive-end bearing with the three planes of unbalance of 10 oz-in per plane. The maximum transmitted bearing force occurs at 6,400 RPM, with a maximum force of 653 lb. From Figure 3.3, it is seen that the maximum force transmitted at the DE bearing occurs at 5,800 RPM. The increase in speed of 600 RPM at which the maximum force occurs is due to the nonlinear effects of the squeeze film damper at NDE bearing. The maximum force for the 1 oz-in at DE was 62 lb, as compared to the 653 lb for the 10 oz-in case. This is still approximately a 10 to 1 ratio. Therefore, it is seen that the unbalance response of the rotor bearing system with the NDE damper is still fairly linear with 10 oz-in of unbalance.

Table 3.1 represents the unbalance response of the rotor with the NDE squeeze film damper, and presents also the bearing and transmitted support forces at 2,400 RPM with the 10 oz-in unbalances at the three planes. The largest rotor amplitude occurs at station 1, which is at the non-drive end. The amplitude is shown to be .75 mils at a phase of 92°. The amplitude at station 14, for example, is only .28 mils at a phase of 105°. The plane angle of 105° near the

Table 3.1 Rotor Response and Bearing Forces Transmitted With 10 oz-in Unbalance At 2,400 RPM

```
**************************************************************************
         Semi-Minor Axis (B): (+) Forward, (-) Backward Precession
******** Steady State Unbalance Response due to Shaft (1) Unbalance ********

  Shaft  1      Speed=     2400.00 rpm  =     251.33 R/S  =       40.00 Hz

********************** Shaft Element Displacements ************************
          =====  X  =====     =====  Y  =====         Elliptical Orbit Data
 stn sub Amplitude Phase     Amplitude Phase         A           B          G

  1   1   .750E-03   92.2     .750E-03  182.2      .750E-03    .750E-03     0.
  2   1   .737E-03   92.1     .737E-03  182.1      .737E-03    .737E-03     0.
  3   1   .708E-03   92.0     .708E-03  182.0      .708E-03    .708E-03     0.
  4   1   .684E-03   92.0     .684E-03  182.0      .684E-03    .684E-03     0.
  5   1   .667E-03   91.9     .667E-03  181.9      .667E-03    .667E-03     0.
  6   1   .631E-03   91.7     .631E-03  181.7      .631E-03    .631E-03     0.
  7   1   .602E-03   91.8     .602E-03  181.8      .602E-03    .602E-03     0.
  8   1   .564E-03   92.2     .564E-03  182.2      .564E-03    .564E-03     0.
  9   1   .522E-03   93.1     .522E-03  183.1      .522E-03    .522E-03     0.
 10   1   .460E-03   94.9     .460E-03  184.9      .460E-03    .460E-03     0.
 11   1   .399E-03   97.3     .399E-03  187.3      .399E-03    .399E-03     0.
 12   1   .347E-03  100.2     .347E-03  190.2      .347E-03    .347E-03     0.
 13   1   .290E-03  104.5     .290E-03  194.5      .290E-03    .290E-03     0.
 14   1   .281E-03  105.4     .281E-03  195.4      .281E-03    .281E-03     0.
 15   1   .250E-03  108.8     .250E-03  198.8      .250E-03    .250E-03     0.
 16   1   .216E-03  113.6     .216E-03  203.6      .216E-03    .216E-03     0.
 17   1   .163E-03  125.0     .163E-03  215.0      .163E-03    .163E-03     0.
 18   1   .126E-03  140.2     .126E-03  230.2      .126E-03    .126E-03     0.
 19   1   .999E-04  164.4     .999E-04  254.4      .999E-04    .999E-04     0.
 20   1   .922E-04  183.2     .922E-04  273.2      .922E-04    .922E-04     0.
 21   1   .944E-04  208.6     .944E-04  298.6      .944E-04    .944E-04     0.
 22   1   .103E-03  222.7     .103E-03  312.7      .103E-03    .103E-03     0.
 23   1   .122E-03  235.9     .122E-03  325.9      .122E-03    .122E-03     0.
 24   1   .168E-03  251.5     .168E-03  341.5      .168E-03    .168E-03     0.

 *** Flexible Support Displacements

 25       .612E-03   91.9     .612E-03  181.9      .612E-03    .612E-03     0.
 26       .233E-04  185.1     .233E-04  275.1      .233E-04    .233E-04     0.
 27       .190E-05   19.2     .190E-05  109.2      .190E-05    .190E-05     0.


****************** Bearing and Support Transmitted Force ******************
  stn      =====  X  =====     =====  Y  =====         Elliptical Orbit Data
  I  J    Amplitude Phase     Amplitude Phase         A           B          G

  4 25    .782E+02  224.9     .782E+02  314.9      .782E+02    .782E+02     0.
 25  0    .781E+02   45.0     .781E+02  135.0      .781E+02    .781E+02     0.
 22 25    .933E+02    5.1     .933E+02   95.1      .933E+02    .933E+02     0.
 15 27    .145E+04   19.2     .286E+01  109.2      .145E+04    .286E+01     0.
 25  0    .154E+00    2.2     .154E+00   92.2      .154E+00    .154E+00     0.
 26  0    .933E+02  185.1     .933E+02  275.1      .933E+02    .933E+02     0.
 27  0    .760E+01   19.2     .760E+01  109.2      .760E+01    .760E+01   135.
**************************************************************************
```

Table 3.2 Rotor Response and Bearing Forces Transmitted With 10 oz-in Unbalance At 8,000 RPM

```
*************************************************************************
        Semi-Minor Axis (B): (+) Forward, (-) Backward Precession
******** Steady State Unbalance Response due to Shaft (1) Unbalance ********

  Shaft  1     Speed=    8000.00 rpm  =    837.76 R/S  =     133.33 Hz

********************** Shaft Element Displacements ************************
          ===== X =====    ===== Y =====        Elliptical Orbit Data
 stn sub Amplitude Phase   Amplitude Phase        A          B          G

  1   1  .299E-02  152.6    .299E-02  242.6     .299E-02   .299E-02    0.
  2   1  .285E-02  151.9    .285E-02  241.9     .285E-02   .285E-02    0.
  3   1  .252E-02  150.1    .252E-02  240.1     .252E-02   .252E-02    0.
  4   1  .226E-02  148.3    .226E-02  238.3     .226E-02   .226E-02    0.
  5   1  .208E-02  146.5    .208E-02  236.5     .208E-02   .208E-02    0.
  6   1  .172E-02  142.2    .172E-02  232.2     .172E-02   .172E-02    0.
  7   1  .146E-02  138.5    .146E-02  228.5     .146E-02   .146E-02    0.
  8   1  .117E-02  133.2    .117E-02  223.2     .117E-02   .117E-02    0.
  9   1  .880E-03  126.1    .880E-03  216.1     .880E-03   .880E-03    0.
 10   1  .524E-03  108.8    .524E-03  198.8     .524E-03   .524E-03    0.
 11   1  .304E-03   69.4    .304E-03  159.4     .304E-03   .304E-03    0.
 12   1  .316E-03   20.6    .316E-03  110.6     .316E-03   .316E-03    0.
 13   1  .448E-03  353.6    .448E-03   83.6     .448E-03   .448E-03    0.
 14   1  .468E-03  351.4    .468E-03   81.4     .468E-03   .468E-03    0.
 15   1  .537E-03  345.3    .537E-03   75.3     .537E-03   .537E-03    0.
 16   1  .596E-03  340.9    .596E-03   70.9     .596E-03   .596E-03    0.
 17   1  .642E-03  336.6    .642E-03   66.6     .642E-03   .642E-03    0.
 18   1  .629E-03  334.9    .629E-03   64.9     .629E-03   .629E-03    0.
 19   1  .584E-03  334.8    .584E-03   64.8     .584E-03   .584E-03    0.
 20   1  .554E-03  336.7    .554E-03   66.7     .554E-03   .554E-03    0.
 21   1  .512E-03  341.9    .512E-03   71.9     .512E-03   .512E-03    0.
 22   1  .488E-03  346.3    .488E-03   76.3     .488E-03   .488E-03    0.
 23   1  .468E-03  351.9    .468E-03   81.9     .468E-03   .468E-03    0.
 24   1  .444E-03    3.6    .444E-03   93.6     .444E-03   .444E-03    0.

 *** Flexible Support Displacements

 25      .175E-02  146.1    .175E-02  236.1     .175E-02   .175E-02    0.
 26      .144E-03  293.8    .144E-03   23.8     .144E-03   .144E-03    0.
 27      .448E-04  260.1    .448E-04  350.1     .448E-04   .448E-04    0.


****************** Bearing and Support Transmitted Force ******************
  stn     ===== X =====    ===== Y =====        Elliptical Orbit Data
  I  J  Amplitude Phase    Amplitude Phase        A          B          G

  4 25  .715E+03  267.1    .715E+03  357.1     .715E+03   .715E+03    0.
 25  0  .714E+03   87.2    .714E+03  177.2     .714E+03   .714E+03    0.
 22 26  .575E+03  113.8    .575E+03  203.8     .575E+03   .575E+03    0.
 15 27  .104E+03   80.1    .104E+03  170.1     .104E+03   .104E+03    0.
 25  0  .147E+01   56.2    .147E+01  146.2     .147E+01   .147E+01    0.
 26  0  .575E+03  293.8    .575E+03   23.8     .575E+03   .575E+03    0.
 27  0  .179E+03  260.1    .179E+03  350.1     .179E+03   .179E+03  135.
*************************************************************************
```

rotor center at the speed of 2,400 RPM is an indication that this speed is above the first critical speed. The drive end of the rotor at station 24 is .17 mils at a phase of 252°.

The squeeze film damper is located at station 4. The motion of the damper is .61 mils at a phase of 92°. It is of interest to note that the absolute amplitude at station 4 is .68 mils at 92°. Therefore, the damper is in phase with the bearing motion and the relative motion of the bearing to the damper is only .07 mils. Therefore, the majority of the motion is due to the motion of the squeeze film damper. Under the column of bearing and support transmitted force, the first tilting pad bearing is located between stations 4 and 25. The bearing force transmitted is 78.2. The damper is located between stations 25 and 0. Zero represents a grounding, or absolute node point. Its bearing force is 78.1. The slight difference between the loads transmitted between the bearing and the damper is due to the mass assumption of the damper bearing.

The seal, which is given by stations 15 to 27, indicates a force of 1,450 lb. This is due to the assumption of the seal stiffness and damping at this speed. Reducing the effective characteristics of the center seal at 2.400 RPM would cause corresponding larger loads to be transmitted to the damper support. However, there would be some increase in amplitude dependent upon the assumption of seal stiffness and damping. The drive-end bearing at station 26 indicates a transmitted force of 93 lb.

Table 3.2 represents the rotor response and bearing forces transmitted with 10 oz-in unbalance at 8,000 RPM. The largest rotor motion occurs at the non-drive end at station 1 and is 3 mils. The phase at station 1 is 153°. At the drive end of the rotor, the amplitude is .44 mils and the motion is out of phase to the 2-station one.

The bearing and support forces transmitted at the non-drive end is 715 lb. The amplitude ratio between the non-drive and drive end bearings is approximately 5. However, the transmitted bearing forces are similar. The force transmitted through the drive end bearing is 575 lb, as compared to 714 at the NDE bearing.

In conclusion, the unbalance response and bearing forces with the large unbalance of 10 oz-in appears to be well behaved and within the linear range. It would appear that a probe at the non-drive end bearing would be the most sensitive to indicate large unbalance at running speed. The center plane unbalance has a minimal effect on the unbalance response at running speed.

Figure 3.7 represents the unbalance response with the unusually large unbalance of 100 oz-in at each of the three planes. This level of unbalance is never expected to occur in practice, but was run to examine the nonlinear response of the squeeze film damper. From Figure 3.7 it can be seen that the largest response at the NDE bearing occurs at 7,400 RPM and is 13 mils.

The mid-span amplitude reaches its maximum value at 2,800 RPM at a value of 5.2 mils. Above 2,800 RPM, the amplitude at the mid-span continues to decrease.

Figure 3.8 represents the transmitted bearing forces to the NDE bearing with the large value of unbalance. Figure 3.9 represents the transmitted forces to the NDE bearing. In this case, it is seen that high bearing forces are transmitted at 8,000 RPM of 12,170 lb at the NDE bearing and 10,160 lb at the DE bearing. The motion generated by this large unbalance distribution is conical at running speed. The calculation of the unbalance response with the 100 oz-in unbalance was for illustrative purposes only. It is felt that even with extremely large values of unbalance, the rotor system would be well behaved.

In summary, it can be concluded that the single squeeze film damper at the NDE bearing will perform very well from the standpoint of unbalance response at both the critical speed and at running speed. The rotor system should be tolerant to moderate values of unbalance. Also, the rotor system should behave very well with the use of 2-plane rigid rotor balancing.

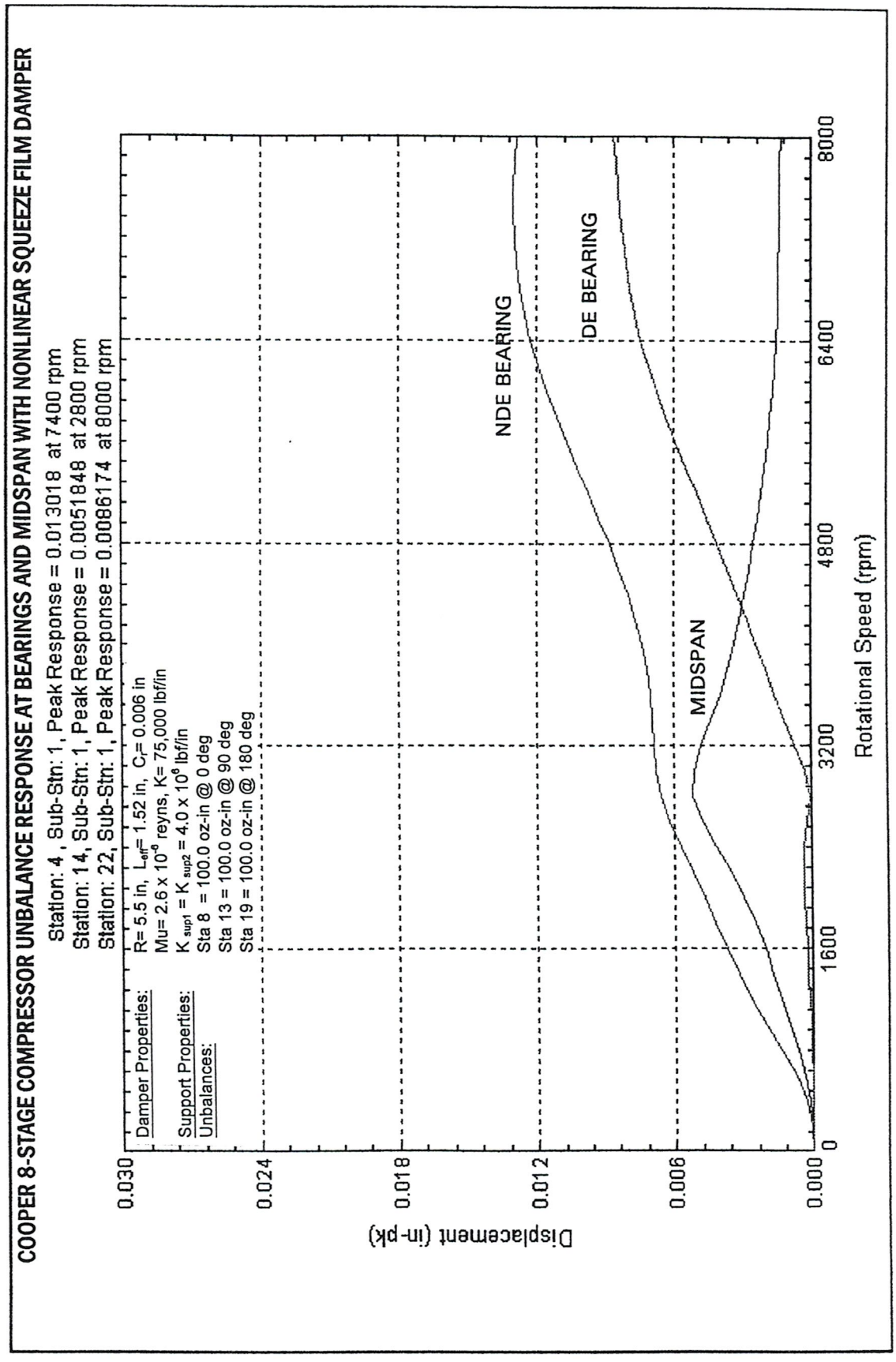

Figure 3.7 Unbalance Response of 8-Stage Compressor in Nonlinear Squeeze Film Damper at NDE With 3 Planes of Unbalance of 100.0 oz-in

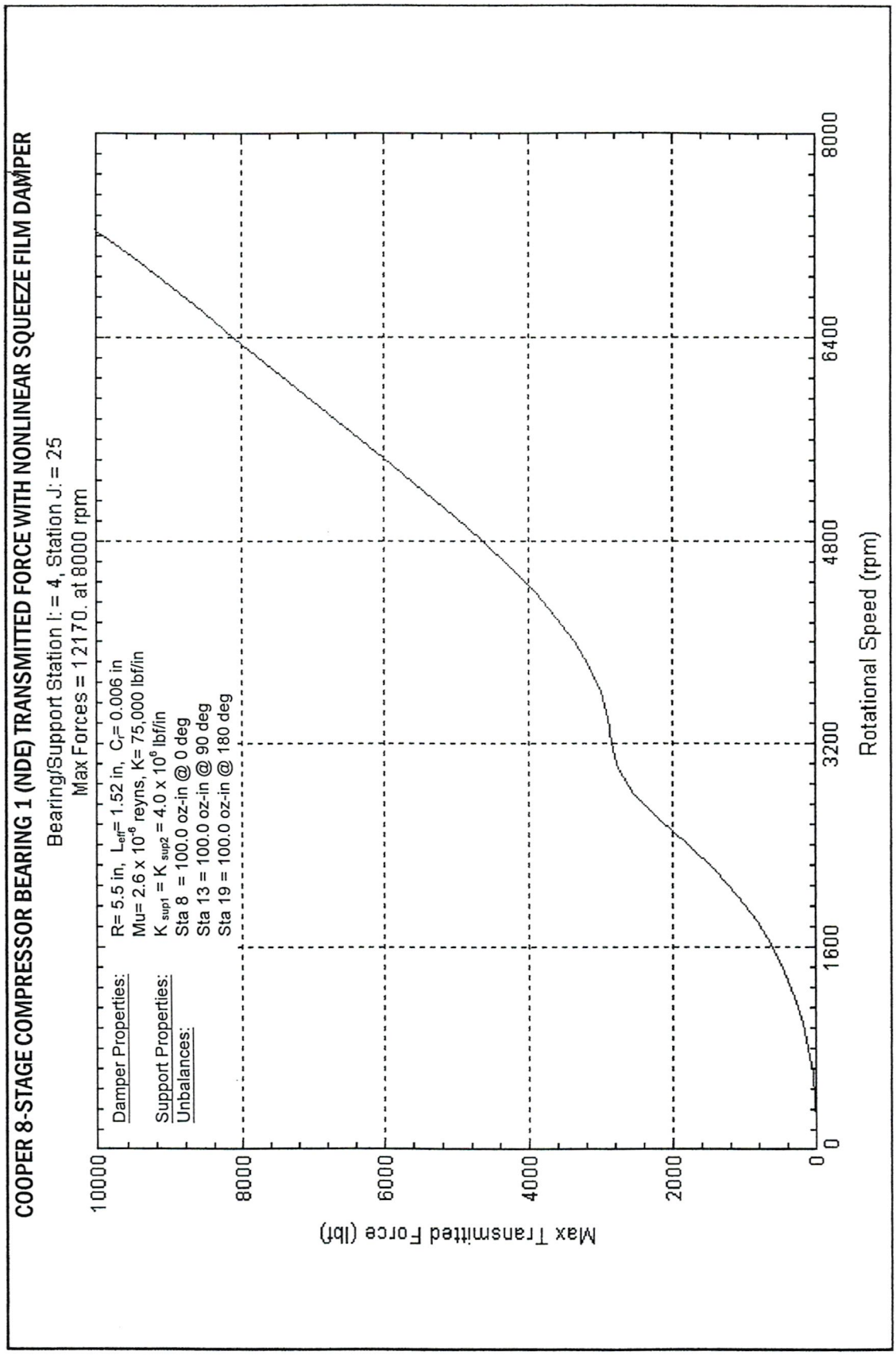

Figure 3.8 Transmitted Bearing Forces to NDE Bearing With Nonlinear Squeeze Film Damper and 3 Planes of Unbalance of 100.0 oz-in